Regional Studies in Marine Science 47 (2021) 101934

Contents lists available at ScienceDirect

Regional Studies in Marine Science

journal homepage: www.elsevier.com/locate/rsma

Assessment of carbon fluxes to coastal area during persistent drought conditions

Mariany Sousa Cavalcante [a], Rozane Valente Marins [a,*], Francisco José da Silva Dias [b], Carlos Eduardo de Rezende [c]

[a] *Laboratório de Biogeoquímica Costeira, Instituto de Ciências do Mar, Universidade Federal do Ceará, Av. Abolição 3207, Fortaleza, CE 60165-081, Brazil*
[b] *Laboratório de Hidrodinâmica Costeira, Estuarina e de Águas Interiores, Instituto de Ciências do Mar, Universidade Federal do Maranhão, Cidade Universitária Dom Delgado, São Luís, Maranhão, CEP: 65080-805, MA, Brazil*
[c] *Centro de Biociências e Biotecnologia, Universidade Estadual do Norte Fluminense, Av. Alberto Lamego 2.000, CEP 28.015-620, Campos dos Goytacazes, RJ, Brazil*

A R T I C L E I N F O

Article history:
Received 7 October 2020
Received in revised form 10 July 2021
Accepted 12 July 2021
Available online 15 July 2021

Keywords:
Dissolved inorganic carbon
Dissolved organic carbon
Particulate organic carbon
Mangrove
Jaguaribe River estuary

A B S T R A C T

This study assesses the seasonal and hydrological factors controlling carbon fluxes and quality of organic matter through the maximum turbidity zone (MTZ) of a tropical semiarid estuary under extreme drought, the Jaguaribe River estuary located in northeast Brazil. Dissolved organic carbon (DOC) and particulate organic carbon (POC) concentrations decreased in the Jaguaribe River estuary during the past ten years, reflecting drought intensification and river damming. DOC and POC behavior were strongly correlated to the freshwater residence time and freshwater fraction. Correlations with Chl-*a* indicated that the biological activity did not regulate DOC but did POC. Stable isotope ratios (δ^{13}C and δ^{15}N) of POC showed that it was predominantly terrestrial-derived, suggesting mangrove as an important POC source. Dissolved inorganic carbon concentrations reflected the seasonal variability of the semiarid climate, being higher in the dry season due to the negative water balance during this period. The Jaguaribe River estuary's MTZ behaved as a retainer of POC (-1.5 $\pm$ 0.2 $\times$ 10^4 tons.year^{-1}), DOC (-1.0 $\times$ 10^5 tons.year^{-1}) and DIC (-4.8 $\pm$ 3.3 $\times$ 10^5 tons.year^{-1}) during the dry season and as an exporter of DOC (+ 2 x 10^4 tons.year^{-1}) and DIC (+1.4 $\times$ 10^5 tons.year^{-1}) in the rainy season. However, the reduced freshwater supply to the estuary resulted in carbon concentrations 50% lower than those reported in 2004 and carbon fluxes smaller than expected for a tropical region. This study indicates that, under a scenario of climatic changes, the intensification of droughts in NE Brazil can further increase carbon retention in the estuary, reducing its exportation to the ocean.

1. Introduction

Rivers worldwide export annually approximately 0.21 Pg (1 Pg = 10^{15}g) of dissolved organic carbon (DOC), 0.20 Pg of particulate organic carbon (POC), and 0.38 Pg of dissolved inorganic carbon (DIC) from land to the ocean (Huang et al., 2012). Estuaries modulate these fluxes due to an intense biogeochemical gradient and being the ultimate land–ocean boundary. In these environments, carbon can suffer microbial, photochemical, and physical transformation processes that affect its amount and quality (Bauer and Bianchi, 2011). It was estimated that estuaries reduce 10% of the global fluvial DOC flux to the ocean (Dai et al., 2012). Arctic estuaries are those that most remove the DOC from riverine waters, reducing the worldwide riverine flux by approximately 3% (Dai et al., 2012).

About 30 to 40% of the organic carbon (OC) buried in marine sediments is of terrestrial origin (Burdige, 2005; Schlünz and Schneider, 2000). Rivers are the main route for the transport of terrestrial OC to the ocean, which contributes approximately 80% of this export (Bianchi, 2011). Any change in fluvial or estuarine inputs can affect the biogeochemical processes occurring in nearshore environments.

Fluvial discharges are controllers of the riverine carbon fluxes (Bauer et al., 2013), but anthropogenic activities have changed them. Although deforestation has increased the fluvial organic carbon flux in the last 30 years in some regions like southeast Asia and Europe (Moore et al., 2013), carbon loads are being reduced globally due to the reservoirs built along rivers that trap terrestrial suspended particulate material (SPM), including carbon, and reduce the freshwater discharges to the coastal areas (Syvitski et al., 2005).

* Correspondence to: Institute of Marine Sciences, Universidade Federal do Ceará, Av. Abolição 3207, Fortaleza, CE 60165-081, Brazil.
E-mail address: rmarins@ufc.br (R.V. Marins).

https://doi.org/10.1016/j.rsma.2021.101934

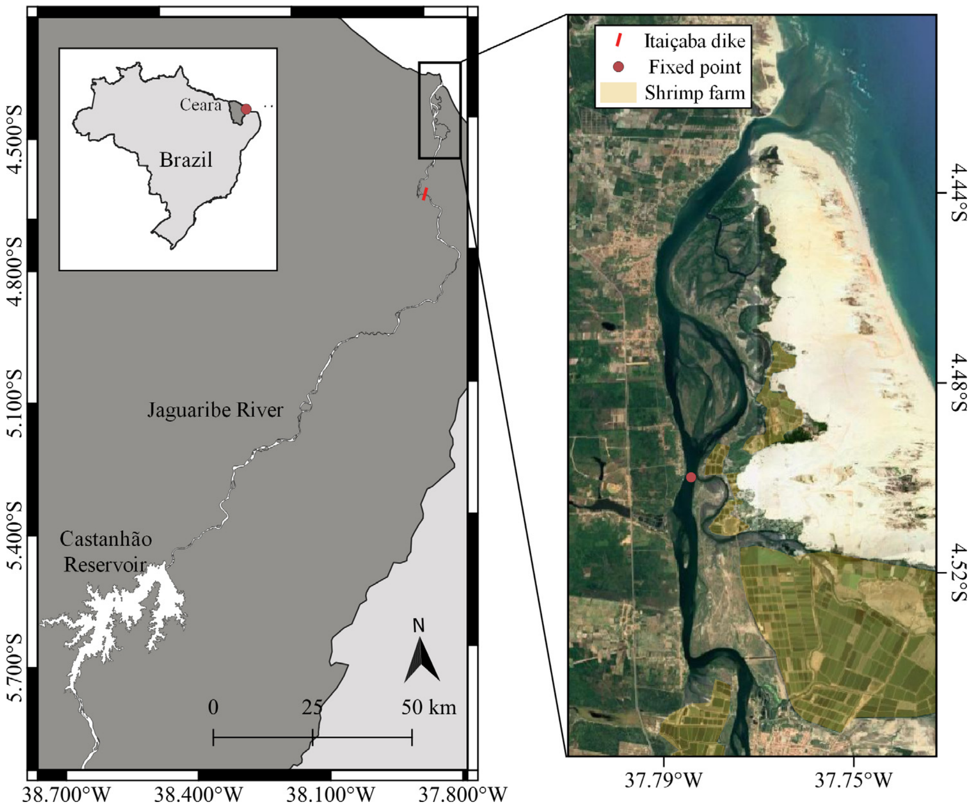

Fig. 1. Location of the study area and the sampling station at the fixed point (FP), in the MTZ of Jaguaribe River estuary, NE Brazil.

Climate is also an essential regulator of terrestrial carbon supply to the coastal zone (Bauer et al., 2013). Seasonality causes variation in carbon fluxes and sources to the estuaries. Usually, carbon fluxes are higher in the wet than in the dry season (Hung et al., 2007). In estuaries under intense seasonal variability of freshwater inflow, terrestrial and riverine sources are predominant during the wet season, while in the dry season, the decrease of freshwater inflow favors the input of marine and estuarine sources (Lebreton et al., 2016; Ye et al., 2017). In the Orinoco River (Venezuela), a reduction of the precipitation by interannual variations resulted in lower carbon fluxes, comparing with data from 20 years ago (Mora et al., 2014). Besides, a single flood event (as a tropical storm) can cause significant increases in carbon export through estuaries located in mountain basins, being responsible for 6%–10% of annual loads (Wu et al., 2013).

Extreme environments are more vulnerable to the effects of climate change and exhibit environmental feedback more evidently (IPCC, 2014). The impacts of climate change in the Arctic have been of big concern in science because the warming at high latitudes has increased the land–ocean fluxes by rivers in this region due to the melting of continental ice (Peterson et al., 2002). Besides, the permafrost thaw, soils rich in organic carbon, have mobilized a substantial fraction of stored carbon to the rivers and coastal regions (Raymond et al., 2007). Similarly, semiarid ecosystems are also extreme environments but somewhat neglected as a major player in the carbon cycle. They are relevant contributors to the global carbon cycle and may even dominate the interannual variability in regions controlled by the El Niño-Southern Oscillation (ENSO) (Zhang et al., 2017).

Drought conditions are increasingly extreme scenarios in semiarid regions, such as in northeastern Brazil, due to the intensification in the frequency and duration of droughts. During the 1600 and 1700 s, drought events occurred from 1 to 3. While in the 2000 s, more than 14 have been recorded (Marengo et al., 2017). The Brazilian semiarid has been pointed out as one of the most affected regions by global climate change (Almagro et al., 2017; Krol and Bronstert, 2007; Zhang et al., 2017), with about 20% reduction in annual rainfall in the past 50 years (Godoy and Lacerda, 2015, 2014). Besides, this region is affected by El Niño that strengthens further the droughts, increasing its vulnerability to climatic changes (Marengo et al., 2017). To mitigate the effects of water scarcity in the Brazilian semiarid, it was built several dams in river basins (Krol and Bronstert, 2007). This is characteristic of the Jaguaribe River, the largest river in Brazil totally inside of the semiarid region (Fig. 1), where there are more than 170 water reservoirs to assure water supply to agriculture, local human settlements, and the city of Fortaleza ($\sim$3.6 million of inhabitants) (Marengo et al., 2017; Marins et al., 2002).

The extended droughts and river damming resulted in the reduction of freshwater flux and the increase of the oceanic forcing in the Jaguaribe River estuary (Dias et al., 2009), mainly during the dry season when the freshwater percentage (FWP) is lower than 5% and the water retention time (RT) is higher than in the rainy season (average of 3.1 days) due to the resistance imposed by tides (Dias et al., 2016). During the rainy season, the FWP in the estuary can reach 90% and the average of RT 0.8 days. However, this is a scenario for years with regular precipitation rates. When precipitation rates are low, the estuarine hydrodynamics is similar to those that occur during the dry season (Dias et al., 2013b). Therefore, the drought intensification and river damming in the semiarid region strengthened, even more, the oceanic forcing in the estuary, causing changes in this major ecosystem, such as the formation of new islands (Godoy and Lacerda, 2013) and the rapid expansion of mangroves (Godoy and Lacerda, 2015).

Mangrove ecosystems have a pantropical distribution and are the major suppliers of terrigenous organic carbon to coastal waters (Prasad and Ramanathan, 2009; Sakho et al., 2015), mainly

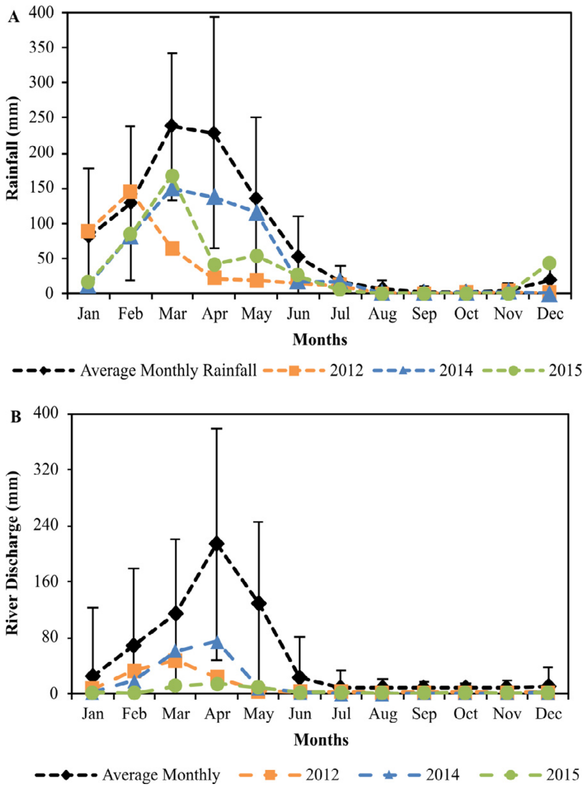

Fig. 2. (A) Monthly rainfall averages with standard deviations between 1980 and 2009 and monthly averages in 2012, 2014 and 2015 over the Jaguaribe basin, NE Brazil (DNOCS, 2017). (B) Monthly river discharge averages with standard deviations between 1980 and 2009 and monthly averages in 2012, 2014 and 2015 in the Jaguaribe River, NE Brazil (DNOCS, 2017).

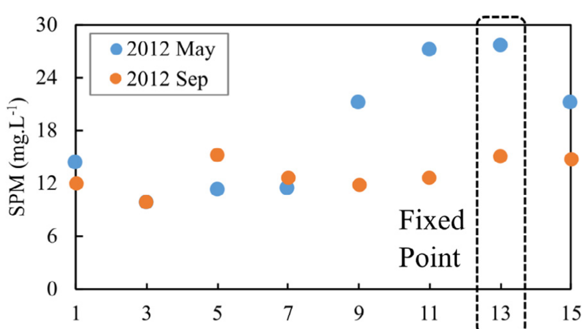

Fig. 3. Spatial distribution of SPM (mg L^{-1}) in the Jaguaribe river estuary in May and September 2012. Identification of the maximum turbidity zone (MTZ).

when the dominant inland vegetation (Caatinga, the dry tropical forests) has low plant biomass and the soils poor in organic matter (OM) as in NE Brazil (Menezes et al., 2012). More than a decade ago, 2004, Mounier et al. (2018) observed remarkable differences in DOC quality and quantity between the dry and rainy seasons in the Jaguaribe River estuary. In the rainy season, DOC concentrations were lower due to the dilution effect by freshwater, and DOC was predominantly of terrestrial origin. While in the dry season, there was the production of young OM in the mangrove-influenced area of the estuary. After that study, the Castanhão reservoir was built in the Jaguaribe river. It is the major dam in the watershed with 6.7 billion m^3 (Santos et al., 2017), which reached maximum capacity in 2010. However, the data published by Mounier et al. (2018) were the last related to the quality and quantity of DOC in the Jaguaribe River estuary.

The mangrove expansion has produced large amounts of highly reactive DOC with abundant complexing sites that can contribute to the metal binding process. In the Jaguaribe river estuary, DOC influences the dynamic of mercury (Hg), creating bioavailable organometallic complexes (Lacerda et al., 2020; Moura and Lacerda, 2018). The Hg complexation is intense during the dry season because the occurrence of the highest water RT favors the interactions between OM and Hg and the accumulation of Hg complexes in the estuarine zone (Lacerda et al., 2020). Whereas during the rainy season, Hg has lower reactivity because it is rapidly exported. Therefore, climate change and river damming have increased the contamination of aquatic biota by Hg in the Jaguaribe river (Lacerda et al., 2020).

The sampling of data from semiarid environments is essential to improve the current carbon fluxes estimates at the land–sea interface. Besides, the main uncertainties in carbon fluxes global estimates are associated with seasonal changes (Huang et al., 2012). This study aimed to (1) measure DOC, POC, and DIC concentration in the Jaguaribe river estuary under a period of extended drought (2012–2017) in different seasons, (2) compare these results with those from before the Castanhão was built to evaluates the changes in carbon dynamic and (3) make the first measures of DOC fluxes of an estuary from the Brazilian semiarid region. It is expected that DOC, POC, and DIC concentrations decrease due to the reduction of riverine discharge due to dam operation and the intensification of drought in semiarid regions. In addition, the contribution of marine-derived OM may increase in the estuary due to the increase of tidal influence.

2. Materials and methods

2.1. Study area

The Jaguaribe River is located in the northeastern equatorial region of Brazil, in the State of Ceará, with 633 km of extension and a drainage basin of 72,043 km^2, being the largest contributor of fluvial waters to the Atlantic Ocean in about 860 km of coastline, between Cabo do Calcanhar and the Parnaíba River Delta (Fig. 1). In this region, where the trade winds of both hemispheres join, the Intertropical Convergence Zone (ITCZ) regulates the climate. The seasonal displacement of the ITCZ southward promotes the occurrence of rains in the Brazilian northeast (Hastenrath, 2012). The Brazilian semiarid is characterized by low (<700 mm $year^{-1}$) and concentrated (4–5 months) precipitation with the prevalence of evaporation (1900 mm $year^{-1}$) over rainfall during most of the year (Schettini et al., 2017). The regional seasonality is defined by a short rainy season from January to May and an extensive dry season from June to December, usually without any precipitation from August to November.

This region is one of the most affected by global climate change (Almagro et al., 2017; Krol and Bronstert, 2007; Zhang et al., 2017), presenting about 20% reduction in annual rainfall in the past 50 years (Godoy and Lacerda, 2014, 2015). During the three-year study period, annual rainfall (Fig. 2A) and river discharge (Fig. 2B) were constantly below the historical average. Consequently, the Castanhão reservoir witnessed a volume reduction from about 85% in November 2011 to about 3.9% in October 2017 due to the absence of rain in the basin, characterizing one of the most extended drought periods observed in the region (DNOCS, 2017; Santos et al., 2017).

Mangroves occupy an area of approximately 7.29 km^2 in the river mouth (Godoy et al., 2018; Godoy and Lacerda, 2014), including the areas recently colonized by them (0.29 km^2). Besides, over 30 km^2 of shrimp farms and urban zones, totaling about 119,000 inhabitants, surround the estuary.

Tides are semidiurnal, with an average tidal wave period of 12 h and 50 min. The estuary's wave propagation curve was estimated using daily water level data provided by the Brazilian Hydrography and Navigation Department for the port of Areia Branca-Termisa (RN) and showed a 2-hour delay relative to that datum (Dias et al., 2009). The mixture of fluvial and coastal water follows a longitudinal gradient of salinity modulated by tides during the dry season and high fluvial discharges during the rainy season when advection transports this mixture to the inner continental shelf (Dias et al., 2013a).

The maximum turbidity is characterized by having high concentrations of SPM compared to more upstream and downstream regions. It is formed in the estuary region where the velocities resulting from convergent movements (river discharge and tidal wave propagation) are practically null, favoring the trapping of SPM (Miranda et al., 2002). Its location varies according to the intensity of the river discharge and tidal range. As river flow increases in the rainy season, the MTZ moves to more downstream regions, and the amount of material generally rises. In addition, the MTZ moves with the tide, being located further upstream at high tide and moving towards the sea at ebb tide (Dyer, 1995). The MTZ frequently occurs at low salinities (1 to 5 g kg^{-1}), in the most upstream estuary zone where the influence of saline intrusion is felt (Dyer, 1995).

Dias et al. (2016) mapped the maximum turbidity zone (MTZ) of the Jaguaribe River estuary between distances of 9 to 15 km from its mouth during the dry season and at ebb tide. While during the rainy season, the MTZ was more extensive, between 5 and 18 km from the mouth at ebb tide. Eschrique (2007) also identified the MTZ at sampling stations between 9 and 18 km from the estuarine mouth during the dry season and high tide. In the dry and rainy seasons of 2012, longitudinal sampling of the suspended matter showed that the location of estuarine MTZ (Fig. 3) was the same in previous years (Dias et al., 2016; Marins et al., 2011), being established as a fixed sampling station for all campaigns performed in this study (Fig. 1) and the depth in this station varies from 2.4 m in ebb tide to 5.5 m in the flood tide.

The processes that occur in the MTZ control the organic matter in the estuary by higher oxidation of OM through its resuspension (Goni et al., 2005) and the intensification of reactions that alter the geochemical partition between DOC and POC (Middelburg and Herman, 2007), for example. Since it is a very dynamic region, many works were developed in the estuarine MTZ of the Jaguaribe river (Dias et al., 2013b, 2016; Mounier et al., 2018). In the present study, the Eulerian sampling was performed to evaluate changes in carbon concentrations over ten years, comparing its results with those reported by Mounier et al. (2018) that adopted this same sampling methodology in the estuarine MTZ. In the Eulerian approach, measurements are made as a function of time at fixed points, the most used in estuarine research (Miranda et al., 2002).

2.2. Sampling and analytical techniques

Given its relevance, three sampling campaigns were conducted at the MTZ of the estuary, two during the dry season (September 2012 and July 2015) and one in the rainy season (May 2014), all at spring tide. The average monthly precipitation of the campaigns was 0, 5, and 116 mm in September 2012, July 2015, and May 2014, respectively. Since July 2015, a strong negative ENSO occurred with increasing intensity in September and October (Alizadeh-Choobari, 2017; Yeoman et al., 2017).

Water collection and hydrochemical measurements were collected every hour, in a fixed point of MTZ (Fig. 1), at subsurface depth (0.5 m) during a tidal cycle of 13 h in each campaign. Dissolved oxygen and pH were measured with a portable YSI (model 85/100 FT) multiparametric probe, while salinity and temperature were measured with a compact temperature and depth probe (Compact CTD model AST D687; JFE Advantech Co., Ltd. Nishinomiya, Hyogo Japan), with a 15 Hz data acquisition frequency. The CTD was used as a standalone unit, and the data were stored in the device's memory. Inconsistent data, generated by systematic and random errors, were deleted. Then, these data gaps were filled using linear interpolation such that only the profiles with a level of interpolation of equal or smaller than 5% were included in the analysis. During pre-processing of the CTD data, spurious data were detected and excluded based on a maximum rate of change of each variable; values exceeding this limit were excluded. We used a Gaussian filter to fill the gaps left by the removal of inconsistent data. After the pre-processing, we evaluated the profiles at 0.5-m depth intervals from the surface to the bottom, and values that differed from the average by more than three times the standard deviation of each block were eliminated (Emery and Thomson, 2001).

Samples were collected in duplicates hourly, a total of 26 samples in each campaign for the analyses of DOC, DIC, POC, and Chl-*a*. Water samples were filtered with pre-combusted (at 450 °C, 12 h) GF/F Whatman fiberglass filters with a 0.7 μm mesh for further analysis of DOC, DIC, POC, and isotopic composition ($\delta^{13}C$, $\delta^{15}N$) of POM (particulate organic matter). Chlorophyll *a* (Chl-*a*) was quantified in the retained pigments in AP40 fiberglass filters until saturation (Grasshoff et al., 1999). It was not possible to evaluate the POC from the rainy season campaign of May 2014 due to loss during transport to the laboratory. The DOC, DIC, and Chl-*a* results were represented by the average of the sampling duplicates (Coefficient of Variation < 10%) to each hour of the tidal cycle.

DOC and DIC were measured with a Hyper TOC Analyzer (Thermo Fisher Scientific, Delft, Netherlands). For the determination of DOC, samples were acidified with HNO_3 (10%) and purged with an inert gas (O_2) to remove inorganic carbon. Next, the organic carbon remaining in the acidified sample (HNO_3) was oxidized by the UV-persulphate (UV-NPOC) photo-oxidation method. The oxidation product (CO_2) of DOC was carried by ultrapure O_2 gas to the non-dispersive infrared analysis detector (NDIR) and then quantified. DIC was measured by the 18% nitric acid oxidation (UV-DIC) methodology that employs acidification of the sample to convert DIC in CO_2 before sending it to infrared non-dispersive detector. Standards used to prepare mixed calibration curves were potassium hydrogen phthalate, calcium carbonate, and hydrogen calcium carbonate, which were diluted to a concentration series adequate for each analysis. The detection limit was 11.63 and 11.42 μmol L^{-1} for DOC and DIC, respectively.

Mangrove leaves (*Rhizophora mangle* and *Avicennia schaueriana*) were collected to measure its isotopic composition ($\delta^{13}C$, $\delta^{15}N$). After being washed, frozen, and lyophilized, the plant samples were milled using a knife mill. The elemental and isotopic composition of carbon in the suspended particulate material and leaves were determined using a Flash 2000 elemental analyzer, with a Conflo IV combined with a Delta V Advantage mass spectrometer (Thermo Scientific IRMS). The analytical control was performed by sampling replicates (Coefficient of Variation < 10%) and certified standards (Elemental Microanalysis Protein Standard), resulting in a 95% precision.

2.3. Assessment of the carbon discharge

Instant current velocities were measured hourly using an ADCP (Sontek/YSI), with a 1500 MHz frequency, towed on a boat moving across the estuarine MTZ; perpendicularly to the water flow to integrate the entire river section. The equipment was programmed for a 5-second burst interval with 0.25 m cells each, at depths between 6 and 7 m in the rainy season and 3 to 4 m in the dry season. The mean transported volume (Tv) or discharge (Q_f) in the mean area of the transversal section (A = A(x, Z)) was calculated as in Eq. (1),

$$T_V = \frac{1}{T}\int_0^T \left[\frac{1}{A}\iint_A \vec{v}.\vec{n}dA\right] dt \quad (1)$$

where $\vec{v} = \vec{v}(x, Z, t)$ is the velocity vector, $\vec{n}$ is the vector normal to section A; T is the time interval of a complete tidal cycle; x is the horizontal distance of the section; and Z is the depth (Miranda et al., 2002). Freshwater percentage and water residence time were calculated based on the flows measured in the transversal section according to Miranda et al. (2002) and Jonge (1992).

The salinity average of the estuarine system was calculated assuming a mixing of marine (V_P) and continental (V_f) water volumes in a semidiurnal tidal cycle when the entire volume was removed from the system during the ebb tide. Therefore, for conservation of mass (volume), Eq. (2) was used to calculate the estuarine mean salinity.

$$S = \frac{V_P}{(V_P + V_f)} S_0 \quad (2)$$

where S is the estuary's mean salinity (g kg^{-1}) during flood and ebb tides, assuming that it is well mixed, and S_0 is the seawater salinity of the adjacent oceanic region (Feistel, 2003; Luketina, 1998; Miranda et al., 2002). The freshwater fraction (V_{fw}) was calculated using Eq. (3):

$$V_{fw} = \frac{V_f}{(V_P + V_f)} \quad (3)$$

The flushing time (T_D) and the Residence Time (RT) represent the time in which one water particle remains within the estuarine system during the flood and ebb tides. According to Ketchum (1950), the T_D for liquid volumes and the water's RT in an estuarine system are the ratio between the volume of freshwater (V_{fw}, m^3) and the discharge (Q_f, m^3 s^{-1}) in the MTZ (Eq. (4)).

$$RT = \frac{V_f}{Q_f} \quad (4)$$

The DOC, DIC, and POC flows were obtained according to the following equation (Eq. (5)):

$$T_{XC} = \iint_A \varphi\vec{v}.\vec{n}dA = \iint_A \varphi.udA = \overline{\varphi}\overline{u}A \quad (5)$$

where T_{XC} is the discharge of carbon fractions [kg s^{-1}], u is the integrated average velocity in the water column (m s^{-1}), φ is the mean concentration of geochemical carbon fractions to each hour, DOC, POC, and DIC (mg L^{-1}), and A is the average area of the section transversal to the direction of the flow (m^2). This methodology has been successfully applied to this estuary (Dias et al., 2016).

2.4. Statistical analysis

Similarities among the campaigns were analyzed using multivariate cluster analysis (Figure A1), considering the parameters evaluated in all of them (hydrochemical and hydrodynamic parameters, Chl-*a*, DOC, and DIC). Two groups were identified: Group 1 included the campaigns performed in the dry season (September 2012 and July 2015) and Group 2 in the rainy season (May 2014). Then, Spearman correlation coefficients were calculated using a raw data matrix to explore possible correlations among variables for rainy and dry separately. A t-test was applied to evaluate differences of DOC and DIC averages between the sampling campaigns.

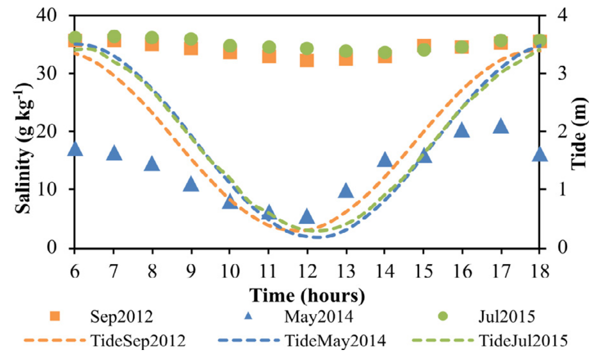

Fig. 4. Temporal variation of salinity in the dry and rainy seasons at the MTZ of the Jaguaribe River estuary.

Table 1
Minimum, maximum, and mean values of salinity (S) and temperature (T).

	S (g kg^{-1})	T (°C)
September 2012	32.2–35.7 **(34.2)**	27.3–29.5 **(28.3)**
May 2014	5.5–21 **(13.7)**	29.7–30.6 **(30.3)**
July 2015	33.1–36.3 **(34.5)**	27.1–29.1 **(28.1)**

3. Results

3.1. Hydrology and water chemistry

Salinity varied between 5.5 and 36.3 g kg^{-1} and exhibited strong seasonal variation, with higher salinity during the dry season (Fig. 4). The thermohaline indexes for the Jaguaribe River estuary (Dias et al., 2013a) were applied to characterize the water masses in the corresponding periods. The salinities were typical of coastal waters (34.5–36) in the dry season and estuarine waters in the rainy season (Table 1).

Instantaneous water discharges measurements varied from 7 to 877 m^3 s^{-1} (Table 2). A bidirectional flux in the MTZ was observed during both seasons, demonstrating a relevant influence of tides in the system (Fig. 5A). In the dry season, water flows during the flood tide were up to 5 times greater than the ebb tide, while in the rainy season (May), these flows were similar (Table 2). Hence, the saline intrusion into the estuary was more intense during dry seasons.

The current speeds (ζ) ranged from 0.25 to 0.71 m s^{-1} (Table 2), and its hourly variation is presented in Fig. 5B. The ζ averages were similar between ebb and flood tides in the September 2012 and July 2015 campaigns, but it was 17% higher in flood than ebb tide in May 2014 (Table 2). In general, there was no statistically significant difference between the average values of ebb tides, except for the year 2012 when presented average values 21% higher. While for the flood, it was possible to observe a reduction of 5% and 18% in May 2014 and July 2015, respectively, compared with September 2012. The residual velocities did not show statistically significant differences (0.04 and 0.05 m s^{-1}, for 2014 and 2015), except for the values observed in 2012 (0.01 m s^{-1}). The residual velocities observed in this study corroborate the values reported by Dias et al. (2016) for the same region of the Jaguaribe River estuary.

Slight variations in the average values of the total currents occurred due to the geomorphological (textual) changes of the bottom, which generate higher friction coefficients, decreasing the current speeds. Dias et al. (2009, 2016) observed that the river has more capacity to transport coarser sediments (medium

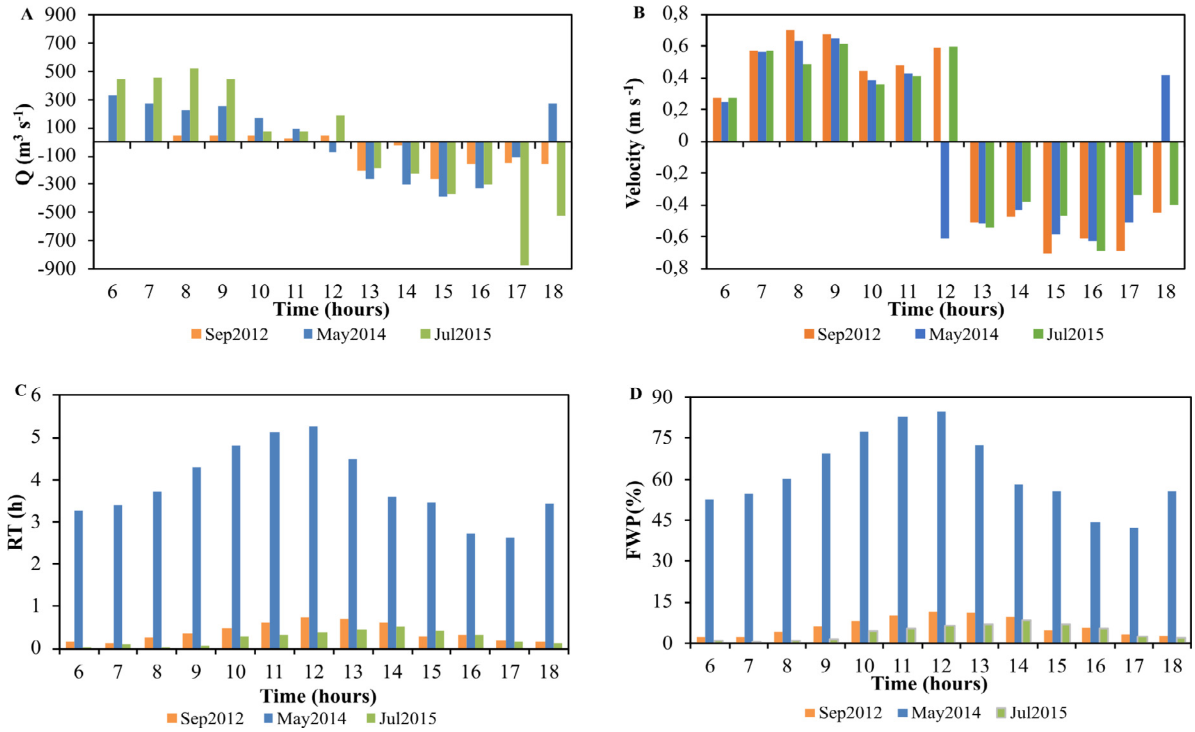

Fig. 5. Temporal variation of (A) water discharge, (B) current velocity, (C) freshwater's residence time (RT) and (D) freshwater percentage (FWP) in the dry and rainy seasons at the MTZ of the Jaguaribe River estuary.

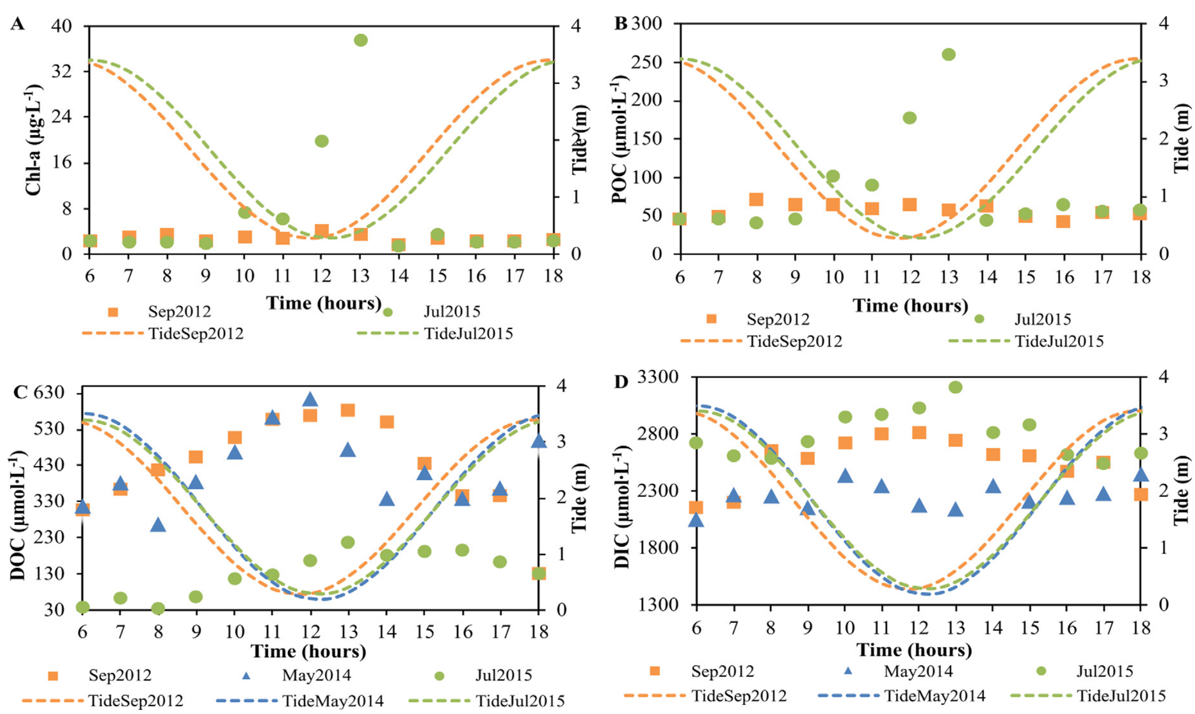

Fig. 6. Temporal variation of (A) Chl-*a*, (B) POC, (C) DOC and (D) DIC concentrations in the dry and rainy seasons at the FP station of the MTZ of the Jaguaribe River estuary.

and fine sand) to the estuary during the rainy season (Godoy and Lacerda, 2014), generating higher friction coefficients near the bottom (Dias et al., 2009). While in the dry season, this capacity is reduced, occurring the grains sedimentation of smaller sizes (Godoy and Lacerda, 2014) and producing less friction near the bottom (Dias et al., 2009). These changes in the bottom granulometry of the Jaguaribe river estuary were observed by Godoy and Lacerda (2014), corroborating with the data presented in this study and with those already described by Dias et al. (2009, 2016).

The total water volume (TV) in the Jaguaribe River estuary varied between 1.6 × 10^5 and 2 × 10^7 m^3. The average of TV was similar between tides in the campaigns of May 2014 and July 2015, but it was one order of magnitude higher in flood than ebb tide in September 2012 (Table 2), indicating a net entrance

Table 2
Minimum, maximum, and mean values of water flow (Q_f), current speeds (ζ), total water volume (TV), freshwater percentage (FWP), residence time (RT).

	Q_f (m^3 s^{-1})		ζ(m s^{-1})		TV (10^5 m^3)		FWP (%)		RT (min)	
	Ebb	Flood_	Ebb	Flood_	Ebb	Flood_	Ebb	Flood_	Ebb	Flood_
September 2012	7–48 **(31)**	27–267 **(160)**	0.27–0.70 **(0.57)**	0.45–0.71 **(0.58)**	1.6–11 **(6.8)**	6.1–60 **(36)**	2.2–11.8 **(6.4)**	2.7–11.2 **(6.2)**	8–44 **(24)**	10–42 **(23)**
	Ebb	Flood	Ebb	Flood	Ebb	Flood_	Ebb	Flood_	Ebb	Flood
May 2014	92–335 **(232)**	73–389 **(244)**	0.25–0.65 **(0.47)**	0.43–0.63 **(0.55)**	21–75 **(50)**	16–87 **(55)**	52–83 **(64.8)**	42.5–84.9 **(59.4)**	197–309 **(241)**	158–316 **(222)**
	Ebb	Flood_	Ebb	Flood_	Ebb	Flood_	Ebb	Flood_	Ebb	Flood_
July 2015	70–552 **(316)**	181–877 **(411)**	0.27–0.61 **(0.47)**	0.34–0.69 **(0.47)**	16–120 **(71)**	40–200 **(92)**	0.5–6.3 **(2.9)**	2.2–8.2 **(5.3)**	2–23 **(11)**	8–31 **(20)**

of marine water. Freshwater RT and the freshwater fraction of the total volume (FWP) were extremely low in the dry season reflecting extensive drought conditions, from 8 to 44 min and from 0.5 to 11.8%, respectively (Fig. 5C and D). While during the 2014 rainy season, there was a 10-fold increase of RT and FWP (158 to 316 min and 42.5 to 84.9% respectively).

3.2. Chl-a, POC, DOC and DIC concentrations in the Jaguaribe River estuary

Chl-*a* concentrations varied from 1.2 to 37.5 μg L^{-1}, displaying a constant pattern most of the time (Fig. 6 A) with maximum values around midday. Mean Chl-*a* concentrations were 2.8 ± 0.6 (1.7 to 4.1), 3.0 ± 2.1 (1.2 to 8.0) and 7.0 ± 10.0 (1.6 to 37.5) μg L^{-1} in September 2012, May 2014 and July 2015 respectively. POC concentrations varied from 41.2 to 261.4 μmol L^{-1} (Fig. 6A), with mean values of 57.6 ±8.1 μmol L^{-1} and 84.1 ±62.2 μmol L^{-1} for the 2012 and 2015 campaigns, respectively. The POC concentrations were practically constant during the tidal cycle in September 2012 (Fig. 6B). In July 2015, an increase of about four times in POC (261.6 μM) happened as well observed to Chl-*a* at the change of the tide. The POC:Chl-*a* ratio varied from 83.6 to 447.6. However, the averages concentrations of each campaign were similar, 254.6 and 232.9 for 2012 and 2015, respectively.

DOC concentrations varied from 34.6 to 614.9 μmol L^{-1}, with mean values of 429.7 ±125.2 μmol L^{-1}, 419.1 ±96.6 μmol L^{-1} and 130.9 ±60.3 μmol L^{-1} for the 2012, 2014 and 2015 campaigns, respectively. There were no differences between DOC concentrations in the first two campaigns ($p > 0.01$), but DOC concentrations in July 2015 were at least three times lower than those observed in May 2014 ($p < 0.01$) and Sep 2012 ($p < 0.01$). The temporal variability of DOC increased in the ebb tide and decreased in the flood tide, showing an inverse relationship with salinity (Fig. 6C). DOC concentrations were higher during the change of the tide. DOC was the dominant fraction of TOC concentrations during the dry season, reaching up to 91%, with mean values of 87 and 61% of TOC in the 2012 and 2015 campaigns, respectively.

DIC concentrations varied from 2057 to 3217 μmol L^{-1}, and mean values of 2558 ± 212 μmol L^{-1}, 2264 ± 113 μmol L^{-1} and 2796 ± 197 μmol L^{-1} for the 2012, 2014 and 2015 campaigns, respectively. DIC concentrations were very variable and statistically different among the three campaigns ($p < 0.01$ for the three t-tests for DIC variability). DIC concentrations were highest during the dry season, mainly in July 2015. Tides notably influenced DIC concentrations in 2012 and 2015 (dry season), but not in the 2014 rainy season (Fig. 6D).

The Spearman correlation analysis (Table 3) showed a significant positive correlation between POC and Chl-*a* during the dry season. POC, DOC, and DIC were positively correlated with FWP and RT and negatively with salinity during the dry season. These correlations were also observed to DOC in the rainy season. DIC did not show a significant correlation with any measured parameters in the rainy season. Table 3 shows only the parameters that showed the most significant correlations with POC, DOC, and DIC. However, it is possible to assess the correlations between all parameters in Tables A1 and A2 of the supplementary materials.

3.3. $\delta^{13}C$ and $\delta^{15}N$ signatures of POC and main endmembers

The $\delta^{13}C$ and $\delta^{15}N$ values of mangroves leaves were of −28.9‰ and 5.5‰ to *Avicennia shaueriana* and −27.6‰ and 3.3‰ to *Rhizophora mangle* respectively ranging in an interval set for the C_3 vegetation (Rezende et al., 1990; Vilhena et al., 2018). Other predominant C_3 plants from the lower drainage basin region as the *Copernicia punifea* and a leguminous presented $\delta^{13}C$ and $\delta^{15}N$ signature of −29.7‰ and 5.7‰ and −27.6‰ and 5.2‰, respectively. The $\delta^{13}C$ and $\delta^{15}N$ signature of OM derived from sediments of fluvial plains (−24.0‰ and 4.8‰) and mangroves (−24.4‰ and 6‰) was more enriched than C_3 from vegetation. The marine endmember has a $\delta^{13}C$ and $\delta^{15}N$ signature of −22.0‰ and 6.7‰ (Carvalho et al., 2017).

The $\delta^{13}C$ signatures of POC ranged from −28.9 to −25‰ (−27.0‰ ± 1.1) during the dry season. The $\delta^{13}C$-POC varied with the tide, presenting relatively more depleted values in low tide than in high tide (Fig. 7A). The $\delta^{13}C$-POC showed a significant negative correlation with RT. FWP. Chl-*a* and POC concentrations and a significant positive correlation with salinity. The $\delta^{15}N$ isotopic composition of the SPM ranged from 2.2 to 6‰ (4‰ ± 1.0), but it seems to be independent of the tidal cycle (Fig. 7B).

4. Discussion

4.1. Reduction of OC supply to the estuary as an effect of drought and river damming

Concentrations of DOC and POC in the Jaguaribe River estuary were typical of estuaries dominated by tides (Middelburg and Herman, 2007) and under similar climate and anthropogenic pressures (Table 4). However, the DOC and POC values presented in this study were more than 50% lower than those reported in 2004 to the Jaguaribe River estuary, when fluorescence matrices of DOM revealed that the DOC was mainly terrestrial-derived (Mounier et al., 2018). Therefore, the decrease in organic carbon concentrations in the estuary pointed to the impact of drought and river damming and has been observed in other regions (Vazquez et al., 2011; Yu et al., 2011).

In 2004. DOC averages were respectively 875 ± 491 and 1.342 ± 209 μmol L^{-1} in the rainy and dry seasons. DOC concentrations were highest during the dry season due to the production of young OM at the mangrove-influenced zone (Mounier et al., 2018). In the present study. DOC did not present this same pattern of variation, being their concentrations similar in the first two campaigns performed in dry and rainy seasons, probably because the low precipitation rate in the rainy season was

Table 3
Spearman correlation of salinity (S), water flow (Q_f), freshwater percentage (FWP) and residence time (RT) with particulate organic carbon (POC), dissolved organic carbon (DOC), dissolved inorganic carbon (DIC), chlorophyll a (Chl-*a*) concentrations, δ^{13}C-POC and POC, DOC and DIC fluxes (T_{POC}, T_{DOC} and T_{DIC}) in the Jaguaribe River estuary ($\alpha = 0.01$). Bold values are significant correlation at $p < 0.01$.

		S	Q_f	FWP	RT	Chl *a*	DOC	DIC	POC
Rainy season (n = 13; $p < 0.01$)	Chl *a*	**−0.67**	−0.43	**0.67**	**0.67**	1.00			–
	DOC	**−0.62**	−0.46	**0.62**	**0.62**	0.33	1.00		–
	DIC	−0.02	−0.25	0.02	0.02	0.14	0.19	1.00	–
	T_{DOC}	0.31	**0.86**	−0.31	−0.313	−0.39	−0.03	−0.19	–
	T_{DIC}	**0.57**	**0.98**	**−0.57**	**−0.566**	−0.50	−0.44	−0.17	–
Dry season (n = 13; $p < 0.01$)	Chl *a*	−0.60	−0.28	0.61	0.62	1.00			
	DOC	**−0.93**	−0.52	**0.93**	**0.91**	0.61	1.00		
	DIC	**−0.89**	−0.57	**0.89**	**0.88**	**0.70**	**0.90**	1.00	
	POC	**−0.68**	−0.37	**0.68**	**0.69**	**0.98**	0.66	**0.78**	1.00
	δ^{13}C	**0.77**	0.51	**−0.77**	**−0.76**	**−0.73**	**−0.77**	**−0.90**	**−0.82**
	T_{DOC}	−0.11	**0.65**	0.12	0.14	0.24	0.20	0.10	0.18
	T_{DIC}	0.59	**1.00**	−0.58	−0.54	−0.23	−0.48	−0.53	−0.32
	T_{POC}	0.02	**0.65**	−0.01	0.03	0.52	0.04	0.06	0.45

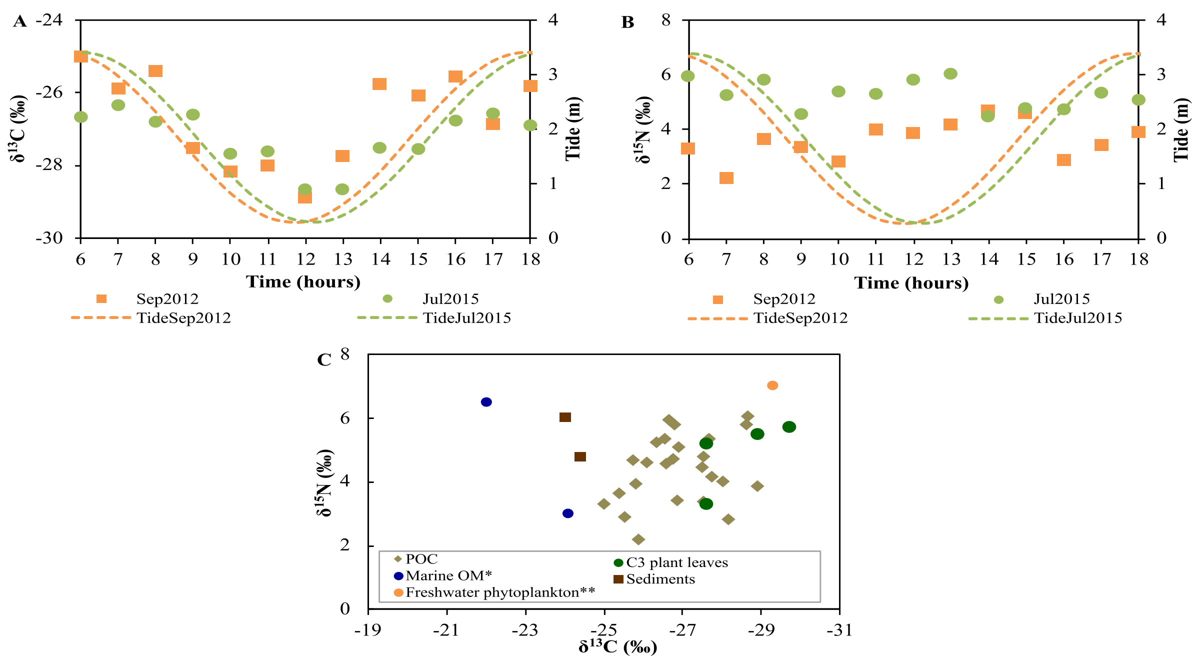

Fig. 7. Temporal variation of (A) δ^{13}C-POC, (B) δ^{15}N-SPM in the dry season at the FP station of the MTZ of the Jaguaribe River estuary and (C) relation δ^{15}N vs δ^{13}C of SPM and endmembers. (Carvalho et al., 2017)* (Ye et al., 2017)**.

Table 4
Anthropogenic pressures, water discharges and carbon concentrations in tropical estuaries.

Estuary (County)	Q_f (m^3 s^{-1})	Anthropic pressures	DOC (µmol L^{-1})	DIC (µmol L^{-1})	POC (µmol L^{-1})	Reference
Wanquan River (China)	69–336	Aquaculture. Urbanization Indutry Damming	75–203	–	25–158	Wu et al. (2013)
Yellow River (China)	600–693	Agriculture Damming	217–258	2.816–3.634	–	Gu et al. (2009)
Tsengwen River (Taiwan)	0–130	Agriculture Damming	100–680	–	30–660	Hung and Huang (2005)
Betsiboka River (Africa)	271	Aquaculture. Deforestation	41.6–125	–	41.6–167	Ralison et al. (2008)
Paraíba do Sul River (Brazil)	–	Agriculture. Livestock Farming. Industry. Urbanization	100–558	–	–	Krüger et al. (2003)
Jaguaribe River (Brazil)	7–877	Damming Agriculture Livestock Aquaculture	35–615	2.057–3.217	41–261	**This study**

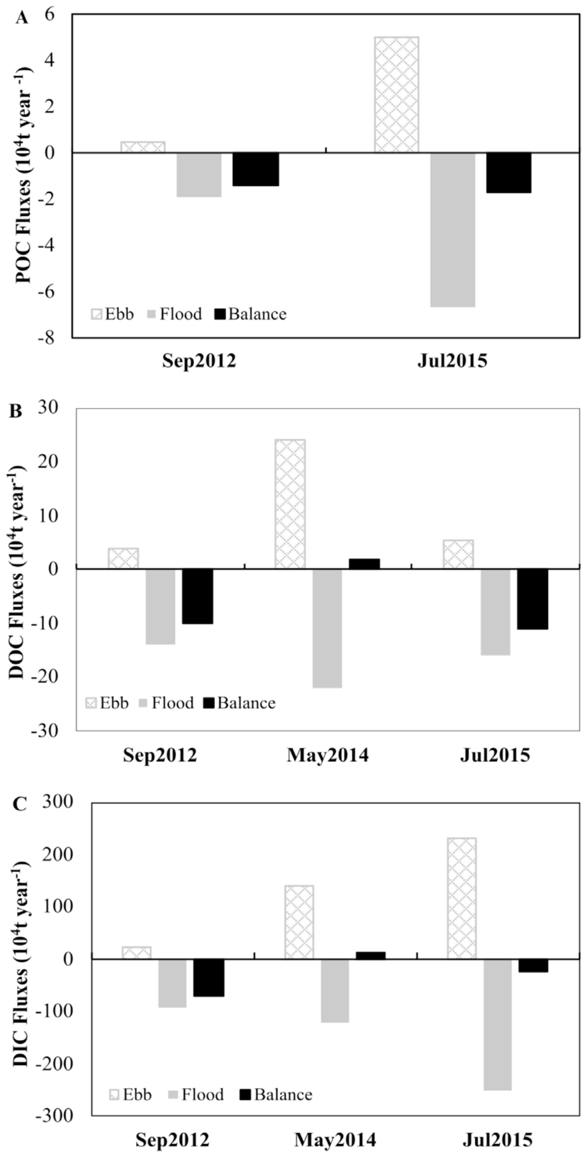

Fig. 8. Fluxes of (A) POC. (B) DOC and (C) DIC through cross-section of MTZ of Jaguaribe river estuary for rainy and dry season. Positive values = exportation; negative values = importation.

not enough to promote the expected variability in DOC values. Besides, the low freshwater RT, compared to those observed previously by Dias et al. (2013b, 2016), might have hindered the accumulation of young OM. DOC concentrations in July 2015 were significantly lower than in the other two campaigns, probable also due to the drought intensification. The distinct DOC and POC values measured in this study showed the vulnerability of the Jaguaribe River estuary to changes in freshwater supply by river damming.

4.2. Drivers and sources of OC in the Jaguaribe River estuary

The positive correlation between POC and Chl-*a* during the dry season indicates that biological activity was relevant POC driver in the estuary (Table 3). However. the small freshwater volume ($<$12%) and high salinity (above 30 g kg^{-1}) in the estuary pointed the freshwater phytoplankton as a minor potential POC source during the dry season, being the marine phytoplankton the chief biological source to POC content.

The POC:Chl-*a* ratio used to discriminate newly produced phytoplankton in POC (POC:Chl-*a* $<$ 200 g g^{-1}) from detrital or degraded material (POC:Chl-*a* $<$ 200 g g^{-1}) (Bianchi et al., 1997; Savoye et al., 2012, 2003) shows that the majority of POC was predominantly detrital or degraded material.

The δ^{13}C-POM in the Jaguaribe River estuary ranged from −28.9 to −25‰ (−27.0‰ ± 1.1), indicating the predominance of terrestrial OM (soils and C_3 plant litter) mixed with marine phytoplankton (Fig. 7C), considering the low freshwater phytoplankton input. The δ^{13}C depletion during the ebb tide occurred due to the greater release of detrital POC from tidal creeks surrounded by mangroves. While during the flood tide, the higher marine forcing caused δ^{13}C-POM enrichment with the input of marine OM, which has δ^{13}C signature of −22.0‰ in the region (Carvalho et al., 2017).

The significant positive correlation between δ^{13}C-POC and salinity showed the relevance of the marine source to the bulk estuarine POC. since this source is more enriched in δ^{13}C. As the negative correlation between δ^{13}C-POC and RT and FWP indicates the contribution of terrestrial OM with the ebb tide. δ^{13}C-POC correlated negatively with POC revealing the relevance of terrestrial input to the increase of POC concentrations.

The SPM generated in the higher portion of the basin is trapped in the Castanhão dam that releases it only when its floodgates are opened (Molisani et al., 2013). The reduction of sediment supply is magnified during intense droughts condition because the estuary became disconnected from the fluvial continuum at Itaiçaba city. Then, during the dry season the SPM originates mainly from the estuary itself and the soils of the lower portion of the watershed (Dias et al., 2013b). As mangroves are the predominant vegetation at the estuary, they are probably the principal OM source to the estuary, as points the similarity between the δ^{13}C and δ^{15}N average values of POC and mangrove leaves. Rezende et al. (1990) showed the mangrove as a significant POC source, varying from 16 to 100% of the total organic carbon flux in a mangrove creek from Sepetiba Bay, and that this contribution was very dependent on tidal amplitude. Therefore, the results obtained in the Jaguaribe River in the current circumstances are very compatible with other regions, characterizing the system as a large tidal creek during the study period.

The non-correlation between DOC and Chl-*a* also suggests weak phytoplankton contribution to DOM and the dominance of terrestrial sources in the dry and rainy seasons. On the other hand, the strong positive correlations between DOC and RT and FWP showed that the estuarine dynamic controlled DOC variability. DOC concentrations decreased during the flood tide and increased during the ebb, showing the strong tidal influence on the estuarine flushing and DOC concentrations. The maximum DOC concentrations in ebb tide might be a result of the higher supply of OM from tidal creeks in ebb tide (Rezende et al., 2007, 1990) as well as the release of mangrove-derived DOC to the water column through tidal pumping of porewater (Kristensen et al., 2008).

4.3. Seasonal and annual DIC increases due to evaporative process

DIC concentrations in the Jaguaribe River estuary were similar to those observed in estuaries of the largest rivers in the world, as the Pearl River estuary (Guo et al., 2008; Jiao et al., 2008; Zhai et al., 2017) (Table 4). The high DIC values in the Pearl River estuary are supported by the high carbonate mineral content (over 80%) in its drainage basin (Guo et al., 2008). In the case of the Jaguaribe River, it has low weathering rates because of low carbonate mineral content in regional geology (Godoy, 2011; Marins et al., 2011). However, the high DIC concentration may happen due mainly to the concentrating effect of high evaporative water loss because of semiarid climate, similarly to a coastal lagoon under Mediterranean climate (Delgadillo-Hinojosa et al., 2008).

In estuaries under dry climate, the balance between precipitation and evaporation plays a relevant role in DIC behavior (Cai et al., 2008). Generally, the higher freshwater discharge in the rainy season results in a dilution of DIC concentrations (Guo et al., 2008), while higher evaporation rates over precipitation increase DIC concentrations during the dry season (Cai et al., 2008). In the Jaguaribe river estuary. DIC reflected the seasonal rainfall variability with higher concentrations during the dry than rainy season. The negative correlation between salinity and DIC (Table 3) during the dry season indicates DIC dilution by seawaters.

DIC concentrations average was 2.284 ± 193 μmol L^{-1} in April 2004 in the estuary's MTZ (Mounier et al., 2018), while it was 2.558 ± 212 μmol L^{-1} and 2.796 ± 197 μmol L^{-1} in September 2012 and July 205 respectively (this study). The increase of DIC concentrations pointed also to the intensification of drought and river damming.

4.4. Carbon flux in the estuarine interface

In drought periods, estuarine waters presented higher salinity than the adjacent ocean because of the low freshwater input, intense evaporation, and strong influence of the tides. In the two campaigns conducted during the dry season, flood tides prevailed in the estuary, generating a hydraulic push by the sea was more intense. Such features resulted in absence of exportation fluxes of POC. DOC, and DIC in the MTZ (Fig. 8A. B. and C). The net landward fluxes (negative fluxes) were -1.4×10^4 tons year^{-1} of POC. -1 x 10^5 tons year^{-1} of DOC and -7.1×10^5 tons year^{-1} of DIC in September 2012. During July 2015, they were -1.7×10^4 tons year^{-1} of POC. -1.1×10^5 tons year^{-1} of DOC and -2.4×10^5 tons year^{-1} of DIC.

During the rainy season, however, the DOC and DIC fluxes were very similar between ebb and flood tides, resulting in the exportation (positive fluxes) of 2×10^4 and 1.4×10^5 tons year^{-1} of DOC and DIC respectively. The average DIC fluxes were one order of magnitude higher than the DOC fluxes. The fluxes were driven by estuarine discharges and not by DOC and DIC concentrations. Probably, there was the export of POC in the rainy season, since that SPM and elements associated with it, such as Hg are exported in the rainy season (Dias et al., 2013b; Lacerda et al., 2013).

The DOC. POC and DIC fluxes in the Jaguaribe River estuary were below the average estimated for tropical rivers (Huang et al., 2012) and estuaries worldwide (Dai et al., 2012) probably because the estimates comprise mostly large rivers that are under positive hydrological balance. The Jaguaribe River estuary, therefore, is more sensitive to environmental changes. Besides, it is under severe drought, related to ENSO events like was observed in the Orinoco River (Mora et al., 2014).

The carbon fluxes through the Jaguaribe River estuary were similar to a semiarid estuary in China (the Yellow River estuary) that is also affected by river damming. The DOC. DIC and POC fluxes of the Yellow River estuary were 3.39×10^4. 3.38×10^5 and 7.0×10^4 ton year^{-1} in the dry season, and 3.04×10^4. 3.57×10^5 and 1.59×10^5 ton year^{-1} in the rainy season, respectively (Gu et al., 2009), pointing a significative effect of drought potentialized by damming.

Estuarine water discharges play a central control in DIC. DOC and POC fluxes (Table 2). If the flow of the Jaguaribe River continues to decrease, carbon export capacity to the ocean will also decrease, as observed in other estuaries which are also under severe drought and river damming (Yu et al., 2011). The reduction of OM supply to the adjacent continental shelf can intensify its oligotrophic characteristic since DOM is a significant source of inorganic nitrogen and phosphorous, as observed by Braga et al. (2018) in the NE Brazil coast. It can threat biological diversity and abundance and, consequently, fishing activities. The low fluxes of DOC through the Jaguaribe River estuary contribute to explain the low DOC levels (mean value of 48.5 μmol L^{-1}) measured in the surface waters of its adjacent continental shelf (Carvalho et al., 2017). Besides, the continuous reduction of fluvial discharge increase POC and DOC retention in the estuary that favors the eutrophication processes, and potentialize carbon association with trace-metal (Lacerda et al., 2020).

5. Conclusions

POC and DOC concentrations decreased by 50% in the Jaguaribe river estuary in the past decade because of the diminishing fluvial flows due to climate change with decreasing of annual rainfall, and river damming. POC and DOC behavior was strongly related to the hydrodynamic parameters such as the freshwater residence time, and freshwater percentage. Besides, estuarine OM was preponderantly terrestrial-derived, and mangroves might be the main OM source to the estuary. The marine phytoplankton contribution was observed through the enrichment of δ^{13}C-POC with the rising tide showed the during the dry season.

DOC and DIC concentration were significantly distinct between the sampling campaigns due to the high interannual variability typical of a semiarid region. DIC concentrations reflected the seasonal variability of the semiarid climate, being higher in the dry season due the concentrating effect caused by the negative water balance.

In the monitored dry seasons, the MTZ of the Jaguaribe River estuary was a retainer of POC. DOC and DIC, while during the rainy season it was an exporter. DIC and DOC fluxes were lower than expected for a tropical river and estuaries worldwide, but similar to other Chinese and South American rivers suffering the influence of dams and decreasing precipitation associated with climate change.

Projections pointing to the intensification of climate change along the northeastern coast of Brazil tend to further reduce carbon fluxes in the region's estuaries, as observed in this study, and may strongly influence the functioning of the estuarine ecosystem and adjacent coastal area.

CRediT authorship contribution statement

Mariany Sousa Cavalcante: Designed the study, Calculated the hydrodynamics parameters and carbon fluxes, Writing of the document. **Rozane Valente Marins:** Designed the study. **Francisco José da Silva Dias:** Designed the study, Calculated the hydrodynamics parameters and carbon fluxes. **Carlos Eduardo de Rezende:** Responsible for POC and isotopic analyses.

Declaration of competing interest

The authors declare that they have no known competing financial interests or personal relationships that could have appeared to influence the work reported in this paper.

Acknowledgments

We acknowledge the support from the PRONEX/FUNCAP/CNPq Proc. Nº PR2-0101-00052.01.00/15 coordinated by Marins. RV that received productivity scholarship from CNPQ Nº 309718/2016-3. MS Cavalcante was funded by the Coordenação de Aperfeiçoamento de Pessoal de Nível Superior - Brasil (CAPES) - Finance Code 001. CE Rezende was funded by Conselho Nacional de Desenvolvimento Científico e Tecnológico – CNPq 305217/2017-8 and FAPERJ Nº E-26/202.916/2017.

Appendix A. Supplementary data

Supplementary material related to this article can be found online at https://doi.org/10.1016/j.rsma.2021.101934.

References

Alizadeh-Choobari, O., 2017. Contrasting global teleconnection features of the eastern Pacific and central Pacific El Niño events. Dyn. Atmos. Ocean 80, 139–154. http://dx.doi.org/10.1016/j.dynatmoce.2017.10.004.

Almagro, A., Oliveira, P.T.S., Nearing, M.A., Hagemann, S., 2017. Projected climate change impacts in rainfall erosivity over Brazil. Sci. Rep. 7, 1–12. http://dx.doi.org/10.1038/s41598-017-08298-y.

Bauer, J.E., Bianchi, T.S., 2011. Dissolved organic carbon cycling and transformation. In: Treatise on Estuarine and Coastal Science. Elsevier Inc., pp. 7–67. http://dx.doi.org/10.1016/B978-0-12-374711-2.00502-7.

Bauer, J.E., Cai, W.J., Raymond, P.A., Bianchi, T.S., Hopkinson, C.S., Regnier, P.A.G., 2013. The changing carbon cycle of the coastal ocean. Nature 504, 61–70. http://dx.doi.org/10.1038/nature12857.

Bianchi, T.S., 2011. The role of terrestrially derived organic carbon in the coastal ocean: a changing paradigm and the priming effect. Proc. Natl. Acad. Sci. USA 108, 19473–19481. http://dx.doi.org/10.1073/pnas.1017982108.

Bianchi, T.S., Baskaran, M., DeLord, J., Ravichandran, M., 1997. Carbon cycling in a shallow turbid estuary of southeast Texas: the use of plant pigment biomarkers and water quality parameters. Estuaries 20, 404–415. http://dx.doi.org/10.2307/1352353.

Braga, E. de S., Chiozzini, V.G., Berbel, G.B.B., 2018. Oligotrophic water conditions associated with organic matter regeneration support life and indicate pollution on the western side of fernando de noronha island - NE. Brazil (3°S). Braz. J. Oceanogr. 66, 73–90. http://dx.doi.org/10.1590/s1679-87592018148306601.

Burdige, D.J., 2005. Burial of terrestrial organic matter in marine sediments: A re-assessment. Glob. Biogeochem. Cycles 19, 1–7. http://dx.doi.org/10.1029/2004GB002368.

Cai, W.-J., Guo, X., Chen, C.-T.A., Dai, M., Zhang, L., Zhai, W., Lohrenz, S.E., Yin, K., Harrison, P.J., Wang, Y., 2008. A comparative overview of weathering intensity and HCO3- flux in the world's major rivers with emphasis on the Changjiang. Huanghe. Zhujiang (Pearl) and Mississippi Rivers. Cont. Shelf Res. 28, 1538–1549. http://dx.doi.org/10.1016/j.csr.2007.10.014.

Carvalho, A.C.O., Marins, R.V., Dias, F.J.S., Rezende, C.E., Lefèvre, N., Cavalcante, M.S., Eschrique, S.A., 2017. Air-sea CO2fluxes for the Brazilian northeast continental shelf in a climatic transition region. J. Mar. Syst. 173, 70–80. http://dx.doi.org/10.1016/j.jmarsys.2017.04.009.

Dai, M., Yin, Z., Meng, F., Liu, Q., Cai, W.-J., 2012. Spatial distribution of riverine DOC inputs to the ocean: an updated global synthesis. Curr. Opin. Environ. Sustain. 4, 170–178. http://dx.doi.org/10.1016/j.cosust.2012.03.003.

Delgadillo-Hinojosa, F., Zirino, A., Holm-Hansen, O., Hernández-Ayón, J.M., Boyd, T.J., Chadwick, B., Rivera-Duarte, I., 2008. Dissolved nutrient balance and net ecosystem metabolism in a Mediterranean-climate coastal lagoon: San Diego Bay. Estuar. Coast. Shelf Sci. 76, 594–607. http://dx.doi.org/10.1016/j.ecss.2007.07.032.

Dias, F.J. da S., Castro, B.M., Lacerda, L.D. de., 2013a. Continental shelf water masses off the Jaguaribe River (4S). northeastern Brazil. Cont. Shelf Res. 66, 123–135. http://dx.doi.org/10.1016/j.csr.2013.06.005.

Dias, F.J.D.S., Castro, B.M., Lacerda, L.D., Miranda, L.B., Marins, R.V., 2016. Physical characteristics and discharges of suspended particulate matter at the continent-ocean interface in an estuary located in a semiarid region in northeastern Brazil. Estuar. Coast. Shelf Sci. 180, 258–274. http://dx.doi.org/10.1016/j.ecss.2016.08.006.

Dias, F.J. da S., Marins, R.V., Maia, L.P., 2009. Hydrology of a well-mixed estuary at the semi-arid Northeastern Brazilian coast. Acta Limnol. Bras. 21, 377–385.

Dias, F.J. da S., Marins, R.V., Maia, L.P., 2013b. Impact of drainage basin changes on suspended matter and particulate copper and zinc discharges to the ocean from the Jaguaribe River in the semiarid NE brazilian coast. J. Coast. Res. 29, 1137–1145. http://dx.doi.org/10.2112/JCOASTRES-D-12-00115.1.

DNOCS. D.N. de O.C. as S., 2017. Açude Castanhão Está Com Apenas 3.9% da Capacidade [WWW Document]. Diário do Nord, URL http://www2.dnocs.gov.br/gab-cs/97-noticias-internas/3733-acude-castanhao-esta-com-apenas-3-9-da-capacidade (accessed 12.4.17).

Dyer, K.R., 1995. Sediment transport processes in estuaries. In: Perillo, G.M.E. (Ed.), Developments in Sedimentology. Elsevier, pp. 423–449. http://dx.doi.org/10.1016/S0070-4571(05)80034-2.

Emery, W.J., Thomson, R.E., 2001. Data analysis methods in physical oceanography. In: Data Analysis Methods in Physical Oceanography. Elsevier Science, Amsterdam, pp. xi–xii. http://dx.doi.org/10.1016/B978-044450756-3/50000-9.

Eschrique, S.A., 2007. Hidrogeoquímica do Fósforo no Estuário do Jaguaribe (CE). Universidade Federal do Ceará.

Feistel, R., 2003. A new extended gibbs thermodynamic potential of seawater. Prog. Oceanogr. 58, 43–114. http://dx.doi.org/10.1016/S0079-6611(03)00088-0.

Godoy, M.D.P., 2011. Mudanças na Sedimentação no Estuário do Rio Jaguaribe (Ce) Devido a Mudanças Nos Usos do Solo. Universidade Federal do Ceará.

Godoy, M.D.P., Lacerda, L.D., 2013. Changes in estuarine islands and rainfall trends in the Jaguaribe River watershed. Ceará State. Brazil. Arq. Ciênc. Mar. 46, 47–54.

Godoy, M.D.P., Lacerda, L.D. de., 2014. River-island morphological response to basin land-use change within the Jaguaribe River Estuary. NE Brazil. J. Coast. Res. 294, 399–410. http://dx.doi.org/10.2112/jcoastres-d-13-00059.1.

Godoy, M.D.P., Lacerda, L.D. de., 2015. Mangroves response to climate change: A review of recent findings on mangrove extension and distribution. Ann. Braz. Acad. Sci. 87, 651–667. http://dx.doi.org/10.1590/0001-3765201520150055.

Godoy, M.D.P., Meireles, A.J. de A., Lacerda, L.D., 2018. Mangrove response to land use change in estuaries along the semiarid coast of Ceará. Brazil. J. Coast. Res. 343, 524–533. http://dx.doi.org/10.2112/jcoastres-d-16-00138.1.

Goni, M.A., Cathey, M.W., Kim, Y.H., Voulgaris, G., 2005. Fluxes and sources of suspended organic matter in an estuarine turbidity maximum region during low discharge conditions. Estuar. Coast. Shelf Sci. 63, 683–700. http://dx.doi.org/10.1016/j.ecss.2005.01.012.

Grasshoff, K., Kremling, K., Ehrhardt, M., 1999. Methods of Seawater Analysis, third ed. Wiley-VCH, Weinheim; New York; Chiester; Brisbane; Singapore; Toronto.

Gu, D., Zhang, L., Jiang, L., 2009. The effects of estuarine processes on the fluxes of inorganic and organic carbon in the Yellow River estuary. J. Ocean Univ. China 8, 352–358. http://dx.doi.org/10.1007/s11802-009-0352-x.

Guo, X., Cai, W.-J., Zhai, W., Dai, M., Wang, Y., Chen, B., 2008. Seasonal variations in the inorganic carbon system in the Pearl River (Zhujiang) estuary. Cont. Shelf Res. 28, 1424–1434. http://dx.doi.org/10.1016/j.csr.2007.07.011.

Hastenrath, S., 2012. Exploring the climate problems of Brazil's Nordeste: A review. Clim. Change 112, 243–251. http://dx.doi.org/10.1007/s10584-011-0227-1.

Huang, T.-H., Fu, Y.-H., Pan, P.-Y., Chen, C.-T.A., 2012. Fluvial carbon fluxes in tropical rivers. Curr. Opin. Environ. Sustain. 4, 162–169. http://dx.doi.org/10.1016/j.cosust.2012.02.004.

Hung, J.-J., Huang, M.-H., 2005. Seasonal variations of organic-carbon and nutrient transport through a tropical estuary (Tsengwen) in southwestern Taiwan. Environ. Geochem. Health 27, 75–95. http://dx.doi.org/10.1007/s10653-004-2291-1.

Hung, J.J., Wang, S.M., Chen, Y.L., 2007. Biogeochemical controls on distributions and fluxes of dissolved and particulate organic carbon in the Northern South China Sea. Deep. Res. II 54, 1486–1503. http://dx.doi.org/10.1016/j.dsr2.2007.05.006.

IPCC, 2014. Climate Change 2014: Synthesis Report. Contribution of Working Groups I. II and III to the Fifth Assessment Report of the Intergovernmental Panel on Climate Change. Core Writi. ed., Geneva. Switzerland.

Jiao, S., Tao, Z., Gao, Q., Liu, K., She, J., Ding, J., Liu, Z., 2008. Stable isotopic composition of riverine dissolved inorganic carbon of the Xijiang river inner estuary. J. Geogr. Sci. 18, 363–372. http://dx.doi.org/10.1007/s11442-008-0363-3.

Jonge, V.N. de., 1992. Tidal flow and residual flow in the Ems estuary. Estuar. Coast. Shelf Sci. 34, 1–22. http://dx.doi.org/10.1016/S0272-7714(05)80123-4.

Ketchum, B., 1950. Hydrografic factors involved in the dispersion of pollutants introduced into tidal wateres. J. Boston Soc. Civ. Eng. 37, 296–314.

Kristensen, E., Bouillon, S., Dittmar, T., Marchand, C., 2008. Organic carbon dynamics in mangrove ecosystems: A review. Aquat. Bot. 89, 201–219. http://dx.doi.org/10.1016/j.aquabot.2007.12.005.

Krol, M.S., Bronstert, A., 2007. Regional integrated modelling of climate change impacts on natural resources and resource usage in semi-arid Northeast Brazil. Environ. Model. Softw. 22, 259–268. http://dx.doi.org/10.1016/j.envsoft.2005.07.022.

Krüger, G.C.T., Carvalho, C.E.V., Ferreira, A.G., Gonçalves, G.M., Truccolo, E.C., Schettini, C.A.F., 2003. Dinâmica de carbono orgânico dissolvido no estuário do rio Paraíba do Sul. R. J. sob diferentes condições de maré e descarga fluvial. Atlântica 25, 27–33.

Lacerda, L.D., Dias, F.J.S., Marins, R.V., Soares, T.M., Godoy, J.M.O., Godoy, M.L.D.P., 2013. Pluriannual watershed discharges of hg into a tropical semi-arid estuary of the Jaguaribe River. NE Brazil. J. Braz. Chem. Soc. 24, 1719–1731. http://dx.doi.org/10.5935/0103-5053.20130216.

Lacerda, L.D. de., Marins, R.V., Dias, F.J. da S., 2020. An arctic paradox: Response of fluvial hg inputs and bioavailability to global climate change in an extreme coastal environment. Front. Earth Sci. 8, http://dx.doi.org/10.3389/feart.2020.00093.

Lebreton, B., Pollack, J.B., Blomberg, B., Palmer, T.A., Adams, L., Guillou, G., Montagna, P.A., 2016. Origin. composition and quality of suspended particulate organic matter in relation to freshwater inflow in a South Texas estuary. Estuar. Coast. Shelf Sci. 170, 70–82. http://dx.doi.org/10.1016/j.ecss.2015.12.024.

Luketina, D., 1998. Simple tidal prism models revisited. Estuar. Coast. Shelf Sci. 46, 77–84. http://dx.doi.org/10.1006/ecss.1997.0235.

Marengo, J.A., Alves, L.M., Alvala, R.C., Cunha, A.P., Brito, S., Moraes, O.L., 2017. Climatic characteristics of the 2010-2016 drought in the semiarid Northeast Brazil region. An. Acad. Bras. Cienc. 1–13. http://dx.doi.org/10.1590/0001-3765201720170206.

Marins, R.V., Freire, G.S.S., Maia, L.P., Lima, J.P.R., Lacerda, L.D. de., 2002. Impacts of land-based activities on the Ceará coast. north-eastern Brazil. In: South American Basins: LOICZ Global Change Assessment and Syntesis of River Catchment - Coastal Sea Interaction and Human Dimensions. LOICZ, Netherlands, p. 212.

Marins, R.V., Paula Filho, F.J., Eschrique, S.A., Lacerda, L.D., 2011. Anthropogenic sources and distribution of phosphorus in sediments from the Jaguaribe River estuary. NE. Brazil. Braz. J. Biol. 71, 673–678. http://dx.doi.org/10.1590/S1519-69842011000400011.

Menezes, R.S.C., Sampaio, E.V.S.B., Giongo, V., Pérez-Marin, A.M., 2012. Biogeochemical cycling in terrestrial ecosystems of the Caatinga Biome. Braz. J. Biol. 72, 643–653. http://dx.doi.org/10.1590/S1519-69842012000400004.

Middelburg, J.J., Herman, P.M.J., 2007. Organic matter processing in tidal estuaries. Mar. Chem. 106, 127–147. http://dx.doi.org/10.1016/j.marchem.2006.02.007.

Miranda, L.B., Castro, B.M., Kjerfve, B., 2002. Princípios em Oceanografia Física de Estuários. EdUSP, São Paulo.

Molisani, M.M., Becker, H., Barroso, H.S., Hijo, C.a.G., Monte, T.M., Vasconcellos, G.H., Lacerda, L.D., 2013. The influence of Castanhão reservoir on nutrient and suspended matter transport during rainy season in the ephemeral Jaguaribe river (CE. Brazil). Braz. J. Biol. 73, 115–123. http://dx.doi.org/10.1590/S1519-69842013000100013.

Moore, S., Evans, C.D., Page, S.E., Garnett, M.H., Jones, T.G., Freeman, C., Hooijer, A., Wiltshire, A.J., Limin, S.H., Gauci, V., 2013. Deep instability of deforested tropical peatlands revealed by fluvial organic carbon fluxes. Nature 493, 660–663. http://dx.doi.org/10.1038/nature11818.

Mora, A., Laraque, A., Moreira-Turcq, P., Alfonso, J.A., 2014. Temporal variation and fluxes of dissolved and particulate organic carbon in the Apure . Caura and Orinoco rivers . Venezuela. J. South Am. Earth Sci. 54, 47–56. http://dx.doi.org/10.1016/j.jsames.2014.04.010.

Mounier, S., Marins, R.V., Lacerda, L.D. de., 2018. Characterization of the Ceara Costal Zone Organic Matter Inputs. archives-ouverts, p. 39.

Moura, V.L., Lacerda, L.D. de., 2018. Contrasting mercury bioavailability in the marine and fluvial dominated areas of the Jaguaribe River Basin. Ceará. Brazil. Bull. Environ. Contam. Toxicol. 101, 49–54. http://dx.doi.org/10.1007/s00128-018-2368-7.

Peterson, B.J., Holmes, R.M., Mcclelland, J.W., Vörösmarty, C.J., Lammers, R.B., Shiklomanov, A.I., Shiklomanov, I.A., Rahmstorf, S., 2002. Increasing river discharge to the arctic ocean. Science (80-.) 2171, http://dx.doi.org/10.1126/science.1077445.

Prasad, M.B.K., Ramanathan, A.L., 2009. Organic matter characterization in a tropical estuarine-mangrove ecosystem of India: Preliminary assessment by using stable isotopes and lignin phenols. Estuar. Coast. Shelf Sci. 84, 617–624. http://dx.doi.org/10.1016/j.ecss.2009.07.029.

Ralison, O.H., Borges, A.V., Dehairs, F., Middelburg, J.J., Bouillon, S., 2008. Carbon biogeochemistry of the Betsiboka estuary (north-western Madagascar). Org. Geochem. 39, 1649–1658. http://dx.doi.org/10.1016/j.orggeochem.2008.01.010.

Raymond, P.A., Mcclelland, J.W., Holmes, R.M., Zhulidov, A.V., Mull, K., Peterson, B.J., Striegl, R.G., Aiken, G.R., Gurtovaya, T.Y., 2007. Flux and age of dissolved organic carbon exported to the Arctic Ocean : A carbon isotopic study of the five largest arctic rivers. Glob. Biogeochem. Cycles 21, 1–9. http://dx.doi.org/10.1029/2007GB002934.

Rezende, C.E., Lacerda, L.D., Ovall, A.R.C., Silva, C.A.R., Martinelli, L.A., 1990. Nature of POC transport in a mangrove ecosystem: A carbon stable isotopic study. Estuar. Coast. Shelf Sci. 30, 641–645. http://dx.doi.org/10.1016/0272-7714(90)90099-D.

Rezende, C.E., Lacerda, L.D., Ovalle, A.R.C., Silva, L.F.F., 2007. Dial organic carbon fluctuations in a mangrove tidal creek in Sepetiba bay. Southeast Brazil. Braz. J. Biol. 67, 673–680. http://dx.doi.org/10.1590/S1519-69842007000400012.

Sakho, I., Mesnage, V., Copard, Y., Deloffre, J., Faye, G., Lafite, R., Niang, I., 2015. A cross-section analysis of sedimentary organic matter in a mangrove ecosystem under dry climate conditions: The Somone estuary. Senegal. J. Afr. Earth Sci. 101, 220–231. http://dx.doi.org/10.1016/j.jafrearsci.2014.09.010.

Santos, J.A., Marins, R.V., Aguiar, J.E., Chalar, G., Silva, F.A.T.F., Lacerda, L.D., 2017. Hydrochemistry and trophic state change in a large reservoir in the Brazilian northeast region under intense drought conditions. J. Limnol. 76, 41–51. http://dx.doi.org/10.4081/jlimnol.2016.1433.

Savoye, N., Aminot, A., Tréguer, P., Fontugne, M., Naulet, N., Kérouel, R., 2003. Dynamics of particulate organic matter δ15N and δ13C during spring phytoplankton blooms in a macrotidal ecosystem (Bay of Seine. France). Mar. Ecol. Prog. Ser. 255, 27–41. http://dx.doi.org/10.3354/meps255027.

Savoye, N., David, V., Morisseau, F., Etcheber, H., Abril, G., Billy, I., Charlier, K., Oggian, G., Derriennic, H., Sautour, B., 2012. Origin and composition of particulate organic matter in a macrotidal turbid estuary: The Gironde Estuary. France. Estuar. Coast. Shelf Sci. 108, 16–28. http://dx.doi.org/10.1016/j.ecss.2011.12.005.

Schettini, C.A.F., Valle-levinson, A., Truccolo, E.C., 2017. Circulation and transport in short. low-inflow estuaries under anthropogenic stresses. Reg. Stud. Mar. Sci. 10, 52–64. http://dx.doi.org/10.1016/j.rsma.2017.01.004.

Schlünz, B., Schneider, R.R., 2000. Transport of terrestrial organic carbon to the oceans by rivers: re-estimating flux- and burial rates. Int. J. Earth Sci. 88, 599–606.

Syvitski, J.P.M., Vörösmarty, C.J., Kettner, A.J., Green, P., 2005. Impact of humans on the flux of terrestrial sediment to the global coastal ocean. Science 308, 376–380. http://dx.doi.org/10.1126/science.1109454.

Vazquez, E., Amalfitano, S., Fazi, S., Butturini, A., 2011. Dissolved organic matter composition in a fragmented Mediterranean fluvial system under severe drought conditions. Biogeochemistry 102, 59–72. http://dx.doi.org/10.1007/s10533-010-9421-x.

Vilhena, M.P.S.P., Costa, M.L., Berredo, J.F., Paiva, R.S., Moreira, M.Z., 2018. The sources and accumulation of sedimentary organic matter in two estuaries in the Brazilian Northern coast. Reg. Stud. Mar. Sci. 18, 188–196. http://dx.doi.org/10.1016/j.rsma.2017.10.007.

Wu, Y., Bao, H., Unger, D., Herbeck, L.S., Zhu, Z., Zhang, J., Jennerjahn, T.C., 2013. Biogeochemical behavior of organic carbon in a small tropical river and estuary. Hainan. China. Cont. Shelf Res. 57, 32–43. http://dx.doi.org/10.1016/j.csr.2012.07.017.

Ye, F., Guo, W., Shi, Z., Jia, G., Wei, G., 2017. Seasonal dynamics of particulate organic matter and its response to flooding in the Pearl River Estuary. China. revealed by stable isotope (δ^{13} C and δ^{15} N) analyses. J. Geophys. Res. Ocean 122, 6835–6856. http://dx.doi.org/10.1002/2017JC012931.

Yeoman, K., Jiang, B., Mitsch, W.J., 2017. Phosphorus concentrations in a Florida Everglades water conservation area before and after El Niño events in the dry season. Ecol. Eng. 108, 391–395. http://dx.doi.org/10.1016/j.ecoleng.2017.07.028.

Yu, H., Wu, Y., Zhang, J., Deng, B., Zhu, Z., 2011. Impact of extreme drought and the Three Gorges Dam on transport of particulate terrestrial organic carbon in the Changjiang (Yangtze) River. J. Geophys. Res. Earth Surf. 116, http://dx.doi.org/10.1029/2011JF002012.

Zhai, W.D., Yan, X.L., Qi, D., 2017. Biogeochemical generation of dissolved inorganic carbon and nitrogen in the North Branch of inner Changjiang Estuary in a dry season. Estuar. Coast. Shelf Sci. 197, 136–149. http://dx.doi.org/10.1016/j.ecss.2017.08.027.

Zhang, A., Jia, G., Epstein, H.E., Xia, J., 2017. ENSO elicits opposing responses of semi-arid vegetation between hemispheres. Sci. Rep. 7, 1–9. http://dx.doi.org/10.1038/srep42281.